How to Cite: Kim, S.V., Baikenov, M.I., Ibishev, K.S., Meiramov, M.G., Ma, Fengyun, & Khamitova, T.O. (2022) Effect of nickel nanopowder on the thermal degradation of coal tar distillate. *Bulletin of the University of Karaganda – Chemistry.* https://doi.org/10.31489/2022Ch2/2-22-19

Article Received: 01 March 2022 | Revised: 28 March 2022 | Accepted: 12 April 2022 | Published online: 25 April 2022

UDC 543.573 https://doi.org/10.31489/2022Ch2/2-22-19

S.V. Kim[*1, 2], M.I. Baikenov[1], K.S. Ibishev[2],
M.G. Meiramov[3], Fengyun Ma[4], T.O. Khamitova[5]

[1]*Karagandy University of the name of academician E.A. Buketov, Karaganda, Kazakhstan;*
[2]*Abishev Chemical and Metallurgical Institute, Karaganda, Kazakhstan;*
[3]*Institute of Organic Synthesis and Coal Chemistry, Karaganda, Kazakhstan;*
[4]*Xinjiang University, Xinjiang, China;*
[5]*Kazakh Agro Technical University named after Saken Seifullin, Nur-Sultan, Kazakhstan*
*(*Corresponding author's e-mail: vanquishV8@mail.ru)*

Effect of nickel nanopowder on the thermal degradation of coal tar distillate

Regularities of influence of nickel nanpowder on the thermal degradation of coal tar distillate were determined using model-free Kissinger, Flynn-Wall-Ozawa and model-fitting Coats-Redfern methods. Coal tar distillate with a boiling point <350 °C was obtained by simple distillation of primary coal tar from the Shubarkol deposit. Nickel nanopowder was used as a catalyst and was added to coal tar distillate in a quantity of 1 % of the mass of the distillate and then the process of thermal degradation of coal tar distillate was conducted at heating rates 5, 10 and 20 °C/min in an inert gas medium. Nickel powder was obtained by high-voltage discharge impact on the dc electrolysis. X-ray diffraction (XRD) analysis showed that the obtained nickel powder has face-centered cubic structure and the average crystallite size calculated by Scherrer equation was ~ 34 nm. Calculations of activation energy were performed via processing of thermogravimetric data. The Kissinger method showed that the activation energy value decreases from 145.19 kJ/mol to 43.65 kJ/mol, by the Flynn-Wall-Ozawa (FWO) method the value decreases from 152.82 kJ/mol to 51.65 kJ/mol, and by the Coats-Redfern method the value decreases from 143.38 kJ/mol to 52.64 kJ/mol. Applicability of these methods are ensured by the high values of correlation coefficients.

Keywords: thermal degradation, nickel, nanopowder, coal tar, distillate, crystallite, thermogravimetric analysis, activation energy.

Introduction

The increasing demands placed on the quality of technological processing of organic raw materials [1] are primarily related to more stringent environmental requirements [2], point to the need for in-depth research on the development of methods for obtaining effective catalytic systems [3]. Studies on the development and application of various nanoheterogeneous catalytic systems for processing of organic raw materials have risen in recent decades [4]. Nickel and its compounds are widely used in the production of various catalytic systems. The processes of aquathermolysis in the presence of iron, cobalt and nickel at 300 °C improves the quality of heavy oil increasing the amount of low-molecular alkanes and reducing content of resins, asphaltenes, polyaromatic compounds, sulfur and nitrogen [5]. For instance, it was found that the pumping hydrogen, nickel-molybdenum nanoparticles in the form of a suspension in a vacuum oil residue at 360 °C in carbonate reservoirs was leading to destruction of almost 50 % of asphaltenes thus causing heavy oil liquefaction and increasing oil recovery [6].

Palladium-nickel phosphide deposited on a silicone-aluminum phosphate molecular sieve contributes to a more orderly mechanism of hydroisomerization of *n*-hexadecane, which leads to a high yield of isomerization products [7].

It is known that coal tar can serve as a raw material for producing gasoline, diesel fuel, etc. For example, the simultaneous use of NiW/γ-Al_2O_3 and NiW/SAPO-11 catalysts in the process of hydrotreating low-temperature resin in a two-stage reactor makes it possible to obtain jet fuel with a freezing point of –51 °C and a high heat value [8]. The catalytic hydrogenation of coal tar in a reactor with two fixed layers in the presence of two catalysts MoNi/γ-Al_2O_3 and of WNiP/γ-Al_2O_3-USY leads to formation of diesel and gasoline fractions with a reduced sulfur and nitrogen content [9]. The Ni/ZSM-5 catalyst obtained by decomposition of nickel tetracarbonyl promotes to a deeper hydrogenation of low-temperature and high-temperature resins, and also contributes to the removal of sulfur and nitrogen [10].

Hydrogenation of a mixture of resin and oil distillation residue with the addition of nickel nitrate and elemental sulfur leads to formation of products which are suitable for coke producing with a more ordered structure and yield greater than with the use of industrial catalysts [11].

Mesoporous spherical NiO-containing catalyst promotes the complete decomposition of anthracene in the hydrogenation process at 300 °C [12]. High conversion of anthracene was observed when hydrogenation process of anthracene in the presence of NiCo supported on chrysotile [13].

NiO supported on chrysotile leads to a significant reduction of activation energy in the process of thermal destruction of primary coal tar/polymeric materials mixture [14].

In this work, the kinetics of thermal degradation of primary coal tar distillate from the Shubarkol deposit without a catalyst and with the addition of nickel nanopowder in a quantity of 1 % of the mass of the organic compound was studied. Nickel nanopowder obtained by the action of a high-voltage discharge on the electrolysis process was used as a catalyst [15].

Experimental

The composition of coal tar distillate obtained by simple distillation of primary coal tar to 350 ºC was determined using an Agilent 7890A gas chromatograph having an Agilent 5975C mass-selective detector. Column parameters Rxi-5ms: length — 30 m, diameter — 0.25 mm, column adsorbent thickness — 0.25 microns, column heating rate 8 °C/min, carrier gas — helium; gas pressure in the column 1.38×10^5 Pa; sample volume 2×10^{-4} cm^3; input mode — split, library — NIST08. The composition of fractions was determined by a semi-quantitative method relative to the peak area. Data processing was carried out using the GS-MSD Data Analysis program.

The surface morphology of the nickel powder was studied using the MIRA 3 TESCAN scanning electron microscope (SEM). Phase composition and crystallite size of nickel powder were determined using X-ray diffraction (XRD) analysis and energy dispersion spectroscopy (EDS). X-ray diffraction analysis was performed on Shimadzu XRD-6000 diffractometer with CuKα-radiation with a wavelength λ = 0.15418 nm. Phase identification was carried out using PDF 4+ databases, as well as the POWDER CELL 2.4 full-profile analysis program.

The average crystallite size of nickel powder was calculated for the largest diffraction peak (111), using the Scherrer equation for spherical particles of cubic symmetry:

$$D = \frac{0.94 \cdot \lambda}{B \cdot \cos\theta}, \qquad (1)$$

where D — is the average crystallite size (nm); λ — is the X-ray diffractometer wavelength (nm); B — is the line broadening at half the maximum intensity (radians); θ — is the Bragg angle. In this equation K — is the numerical factor depends on crystallite shape and in our case K = 0.94.

Thermogravimetric analysis was performed on the Labsys Evo TG-DTA/DSC 1600 °C derivatograph (Setaram, France) at heating rates of 5, 10 and 20 °C/min, in nitrogen atmosphere.

Since the distillate is a liquid organic mass, it was mixed with Al_2O_3 in order to avoid boiling and splashing. Al_2O_3 was pre-calcined at 600 °C for 4 hours. Distillate with the mass of 5 g was mixed with Al_2O_3 in the ratio of 1:4.

Sample containing nickel powder was prepared as follows: 5 g of the distillate was mixed with the 0.05 g (1 % of distillate weight) nickel powder and this mixture was thoroughly stirred. Then Al_2O_3 was added to obtained mixture with the same ratio as in the case of sample without nickel powder. $10\cdot10^{-3}$ g of obtained mixture was taken for thermal analysis.

The kinetic parameters were determined based on the assumptions that the rate of transformation of a substance is a linear function depending on the temperature T and conversion ω [16]:

$$\frac{d\omega}{dt} = k(T)\, f(\omega), \qquad (2)$$

where ω — is the conversion which can be found from the relation [17, 18]:

$$\omega = \frac{m_i - m_t}{m_i - m_e}, \qquad (3)$$

where m_i — is the initial mass sample; m_t — is the mass at time; m_e — is the final mass.

The basic equation for non-isothermal conditions has the form:

$$\frac{d\omega}{dt} = \frac{Z}{\beta}\exp\left(-\frac{E}{RT}\right) f(\omega), \quad (4)$$

where Z — is the pre-exponential or frequency factor (sec^{-1}); R = 8.314 kJ/(mol·K) — is the universal gas constant; T — is the temperature (K); E — is the activation energy (kJ/mol); β — is the heating rate.

The Kissinger and Flynn-Wall-Ozawa model-free methods and the Coats-Redfern model method were used to evaluate the effect of nanosized nickel powder on changing the activation energy.

The calculation of kinetic parameters by the Kissinger iso-conversion method is based on the equation [19]:

$$\ln\left[\frac{\ln\beta}{T^2}\right] = \ln\left[\frac{ZR}{E}\right] - \frac{E}{RT}. \quad (5)$$

The slope of the straight line plotted in coordinates $\ln\left[\frac{\ln\beta}{T^2}\right]$ versus $\left(\frac{1000}{T}\right)$ allows the activation energy E to be computed.

For the calculation kinetic parameters according to the Flynn-Wall-Ozawa model-free method was used the following equation, taking into account the Doyle's approximation [20]:

$$\ln\beta = \ln\left[\frac{Z\cdot E}{R\cdot g(\omega)}\right] - 5.331 - 1.052\frac{E}{RT}. \quad (6)$$

("1000"/"T") along the slope of the straight line, the activation energy E was found.

A plot of $\ln\left[\frac{g(\omega)}{T^2}\right]$ versus $\left(\frac{1000}{T}\right)$ gives a straight line with the slope which allows the determination of the activation energy E.

A Coats-Redfern method, which refers to model-fitting methods was also applied to determine the activation energy E [21]. The equation used in this method is of the form:

$$\ln\left[\frac{g(\omega)}{T^2}\right] = \ln\left[\frac{ZR}{\beta E}\left[1-\frac{2RT}{E}\right]\right] - \frac{E}{RT}. \quad (7)$$

All calculations are made under the condition that the reaction order is n = 1.

Results and Discussion

According to the result of the chromatography-mass spectrometric analysis, it was found that the the obtained coal tar distillate comprised: alkanes (C_{12}–C_{20}), alkenes (C_{13}–C_{16}), cycloalkanes (C_7–C_{11}), alkylbenzenes (C_7–C_{11}), bicyclic alkanes, phenylcycloalkanes, naphthalenes (alkylnaphthalenes), biphenyls (alkyl biphenyls), phenols and O-, N- and S-containing compounds. The composition of distillate is shown in Table 1.

Table 1

The composition of the obtained coal tar distillate (< 350 ºC)

№	Compound	Area, %	№	Compound	Area, %
1	2	3	4	5	6
1	3-Methylpyridine	0.15	12	5-Decanone	0.20
2	1,3-Dimethyl benzene	0.11	13	2-Ethyl phenol	5.4
3	3,5-Dimethylpyridine	0.21	14	1,3-Cyclopentanedione, 2-chloro	0.19
4	Phenol	3.78	15	3,5-Dimethyl phenol	3.32
5	3-Methylbenzyl mercaptan	0.21	16	Triquinacene	0.53
6	1-Methylpropyl benzene	0.14	17	2,6-Dimethylanisole	0.27
7	2-Cyclopenten-1-one, 2,3-dimethyl	0.27	18	3-Ethyl phenol	1.90
8	1-Propynyl benzene,	0.13	19	(3-Methyl-2-butenyl) benzene	0.22
9	2-Methyl phenol	3.21	20	1,2-Benzenediol	0.52
10	4-Methyl phenol	7.50	21	4,7-Dimethylbenzofuran	0.28
11	2,6-Diethylpyridine	0.18	22	2-Propyl phenol	0.43

Continuation of Table 1

1	2	3	4	5	6
23	2-Ethyl-6-methyl phenol	1.03	55	1-Naphthalenol	1.15
24	2,3-Dimethylanisole	0.14	56	2(1H)-Quinolinone, 4,8-dimethyl	1.76
25	1-Ethyl-4-methoxy benzene	1.05	57	1,6,7-Trimethyl naphthalene	2.5
26	2,4-Dimethylanisole	1.84	58	1,4,6-Trimethyl naphthalene	0.84
27	1,2-Benzenediol, 3-methyl-	1.35	59	4,6,8-Trimethyl azulene	1.47
28	3,4-Dimethylanisole	0.48	60	1-Heptadecene	1.35
29	Cyclohexane, 1,2,3-trimethyl-, (1 alpha., 2.beta., 3.alpha.)	0.38	61	Heptadecane	5.11
30	1H-Indene, 2,3-dihydro-4,7-dimethyl	0.27	62	1-methyl-7-(1-methylethyl) naphthalene	0.70
31	3,5-dimethyl octane	0.76	63	1-Naphthalenol, 2-methyl-	2
32	1,2-Benzenediol, 4-methyl	1.45	64	Ethanol, 2-(5-amino-6-chloropyrimidin-4-ylamino)-	1.32
33	2-Methyl naphthalene	3.08	65	1-Methyl-7-(1-methylethyl) naphthalene	0.43
34	1-(2-Hydroxy-5-methylphenyl) ethanone	0.40	66	Methyl diisopropylphosphoramioridite	0.51
35	2-Methyl-5-(1-methylethyl) phenol	0.51	67	1,6-Dimethyl-4-(1-methylethyl) naphthalene	1.41
36	6,7-Dimethyl-1,2,3,4-tetrahydronaphthalene	0.54	68	9-Methoxyfluorene	0.53
37	1H-Inden-5-ol, 2,3-dihydro	0.86	69	1,4-Dihydro-2,5,8-tri methyl naphthalene	1.04
38	1,3-Benzenediol, 4-ethyl	0.71	70	1-Naphthol, 6,7-dimethyl-	1.19
39	6-Methyl-4-indanol	0.29	71	1-Naphthol, 5,7-dimethyl-	0.41
40	2-Ethyl-3-methoxypyrazine	1.61	72	N-Methoxy-2-carbomethoxy-2-carbeth oxyaziridine	0.33
41	1-(2,4-Dimethylphenyl) ethanone	0.51	73	N-Methyl-1-hydroxycarbazole	0.64
42	1,2,3-Trimethylindene	0.71	74	3-Methyl tetradecane	3
43	1,3-Cyclohexanedione, 5-isopropyl	0.45	75	Phenanthrene	0.35
44	1-(2,4-Dimethyl-furan-3-yl) ethanone	2.75	76	6-Methoxy-2-(1-buten-3-yl) naphthalene	0.32
45	1,2,3,4-Tetrahydro-1,1,6-trimethyl naphthalene	1.08	77	3,4-Dimethyl(1H)pyrrole, 2-[(3,4-d imethyl-[2H]-pyrrol-2-ylidene	0.24
46	2,7-Dimethyl naphthalene	1.28	78	Trifluoroacetoxy hexadecane	0.19
47	2-Allyl-4-methylphenol	0.32	79	Eicosane	2.45
48	2,3-Dimethyl naphthalene	3.19	80	7-Hydroxycadalene	0.20
49	1-(2,5-Dimethylphenyl) ethanone	2.06	81	1-Hexadecene	0.24
50	1-Pentadecene	0.70	82	Heneicosane	1.58
51	Pentadecane	1.57	83	Octadecyl trifluoroacetate	0.26
52	Acenaphthene	0.58	84	1-Methyl-7-(1-methylethyl) phenanthrene	0.41
53	3-Ethyl-1,2,4,5-tetramethyl benzene	0.90	85	11-Tricosene	0.16
54	2,3,6-Trimethyl naphthalene	0.64	86	Hentriacontane	2.3

SEM analysis (Fig. 1) showed that the nickel powder consist of nanoscale particles with a form is close to a spherical forming aggregates. The presence of small amount of oxygen and carbon were found by EDS (Fig. 1).

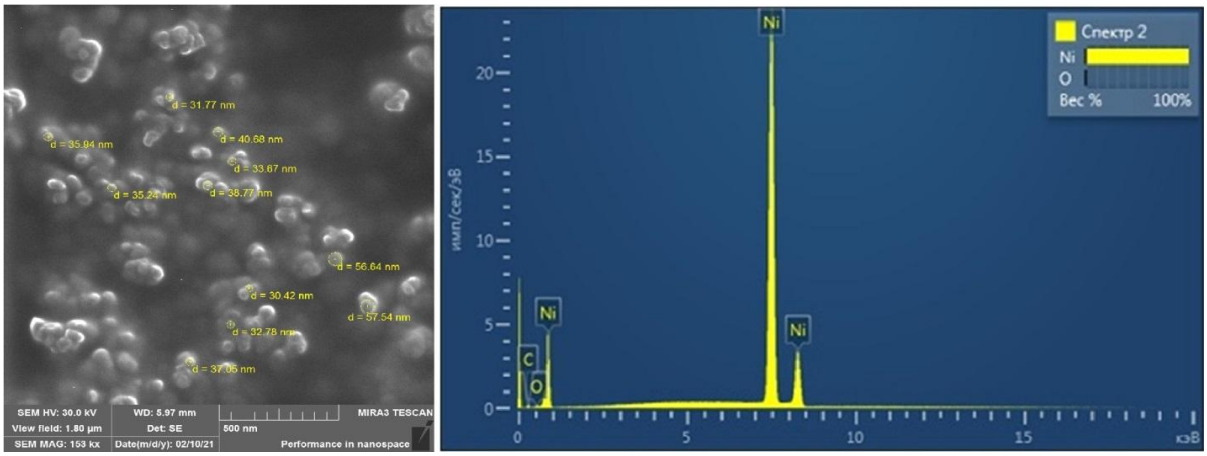

Figure 1. SEM image and EDS of nickel powder

On the XRD pattern (Fig. 2) basic peaks with the Miller indices (111), (200) and (220) were observed at the appropriate values of interplanar distances 2.034 Å, 1.762 Å and 1.246 Å. These parameters were in accordance with face-centered cubic structure. Calculation using the Equation (1) showed that medium crystallite size was approximately 34 nm.

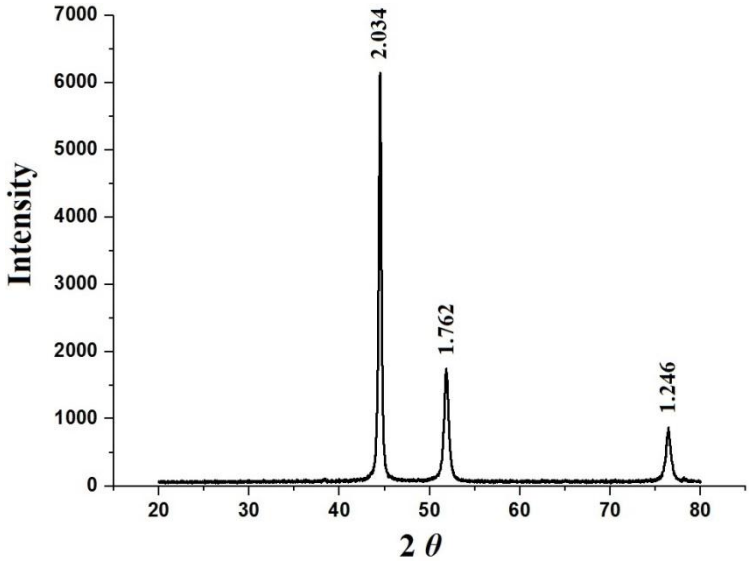

Figure 2. Diffraction pattern of the nickel powder

The effect of heating rate 5, 10 and 20 °C/min on weight loss (%) is presented in the Figure 3.

The values of activation energies calculated by the Kissinger method showed that high correlation coefficients R^2 = 0.966–0.9915 were received for the conversion ω in the range 20–60 % for thermal decomposition of primary coal tar distillate without a catalyst (Table 1).

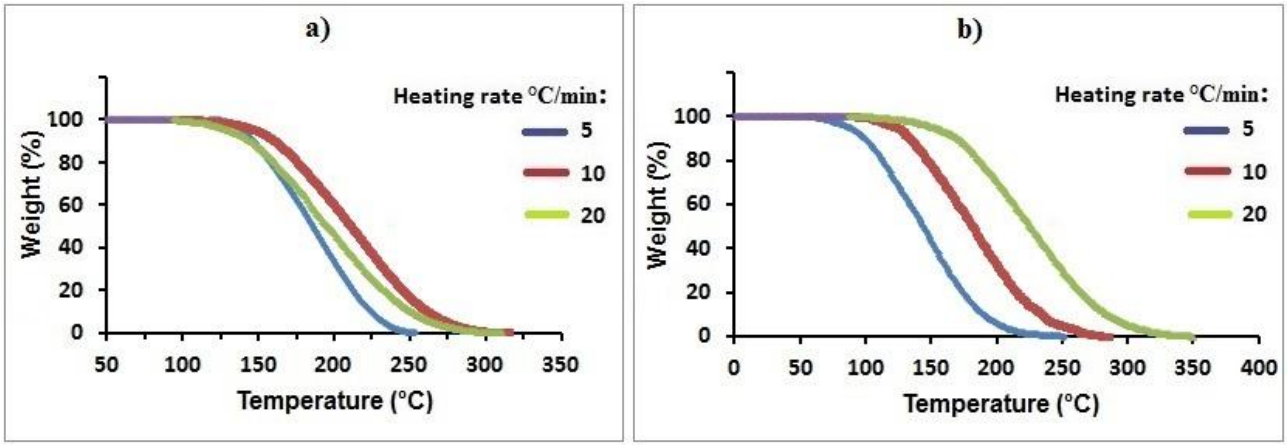

a — without a catalyst; *b* — in the presence of nickel powder

Figure 3. The effect of heating rate 5, 10 and 20 °C/min on weight loss (%)

At a heating rate of 5 °C/min, a temperature shift of the start of degradation is observed from ~140 °C without a catalyst versus ~90 °C in the presence of nickel powder. For the heating rate 10 °C/min, the shift was from ~150 °C to ~125 °C. And for the heating rate 20 °C/min the temperature of the start of degradation was ~125 °C without the catalyst and ~160 °C in the presence of nickel powder.

The plots obtained by the Kissinger method are shown in Figure 4.

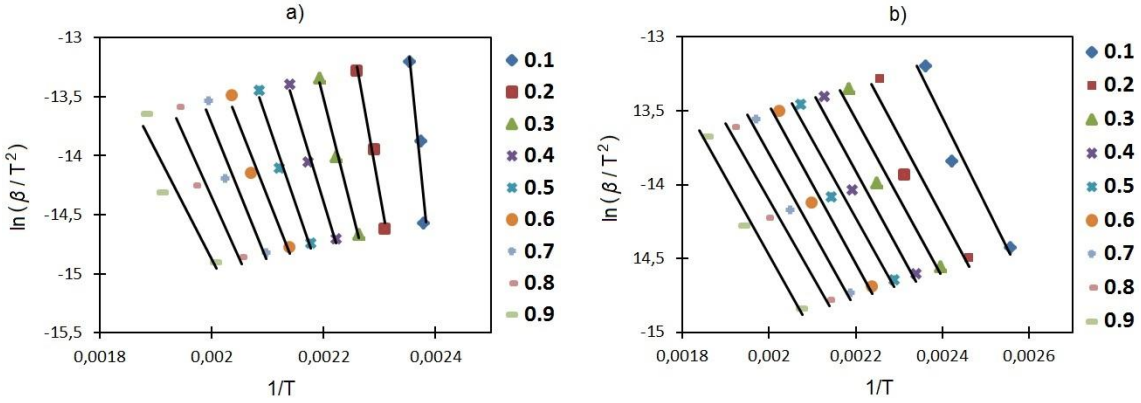

a — without a catalyst; *b* — in the presence of nickel powder

Figure 4. Kissinger approximation plots of thermal degradation of primary coal tar distillate

The average value of the activation energy E_a = 145.19 kJ/mol was calculated from the activation energy values for conversion (ω) in the range 0.2–0.6 with correlation coefficients $R^2 \geq 0.96$.

Table 2

Calculation of activation energy at various conversions by the Kissinger method

Without a catalyst									
Conversion (ω)	0.1	0.2	0.3	0.4	0.5	0.6	0.7	0.8	0.9
Correlation coefficient (R^2)	0.8481	0.9847	0.9915	0.9857	0.9832	0.963	0.9352	0.9177	0.8913
Activation energy (E_a, kJ/mol)	392.98	220.04	158.42	131.9	114.97	100.62	96.77	87.07	76.62
In the presence of catalyst									
Conversion (ω)	0.1	0.2	0.3	0.4	0.5	0.6	0.7	0.8	0.9
Correlation coefficient (R^2)	0.9403	0.9177	0.9359	0.9404	0.9514	0.9606	0.9682	0.9667	0.9762
Activation energy (E_a, kJ/mol)	49.1	45.53	44.72	44.57	43.54	44.52	43.75	42.69	43.76

When calculating by the Kissinger method for the thermal decomposition of coal distillate with the addition of nanoscale nickel powder in a quantity of 1 % of distillate weight, the activation energies with correlation coefficients $R^2 \leq 0.98$ were obtained for all the range of ω = 0.1–0.9 (Table 2). The average activation energy E_a = 43.65 kJ/mol was calculated from the activation energies obtained in the range ω = 0.5–0.9 with R^2 = 0.9514–0.9762.

Linear relationships obtained by the Flynn-Wall-Ozawa method are illustrated in Figure 5.

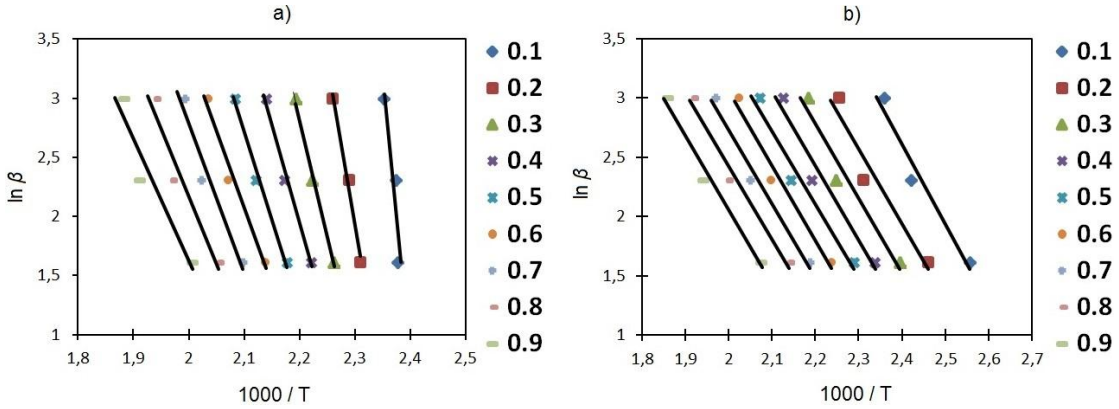

a — without a catalyst; *b* — in the presence of nickel powder

Figure 5. Linear relationships obtained by the Flynn-Wall-Ozawa method

The calculation of activation energies at various conversions by the FWO method (Table 3) showed that the highest correlation coefficients R^2 were in the range of conversions ω = 0.2–0.6 for thermal decomposition of primary coal tar distillate without a catalyst. The average value of activation energy were calculated for ω in the range 0.2–0.6 and accounted for E_a = 152.82 kJ/mol.

Table 3

Calculation of activation energy at various conversions by the FWO method

Without a catalyst									
Conversion (ω)	0.1	0.2	0.3	0.4	0.5	0.6	0.7	0.8	0.9
Correlation coefficient (R^2)	0.8527	0.9856	0.9922	0.9872	0.9852	0.9679	0.9441	0.9302	0.9098
Activation energy (E_a, kJ/mol)	400	227.32	165.89	122.77	140.27	108.58	104.88	95.39	85.15
In the presence of catalyst									
Conversion (ω)	0.1	0.2	0.3	0.4	0.5	0.6	0.7	0.8	0.9
Correlation coefficient (R^2)	0.9527	0.9364	0.9511	0.9549	0.9636	0.9705	0.9764	0.9756	0.9826
Activation energy (E_a, kJ/mol)	55.85	52.57	51.97	52	51.15	51.31	51.74	50.88	51.2

Calculation by the FWO method for thermal decomposition of distillate with the addition of nickel powder (in a quantity of 1 % of distillate weight) showed that the values of activation energies were received at correlation coefficients $R^2 < 0.99$ for all the range of conversion ω = 0.1–0.9. The average activation energy E_a = 51.65 kJ/mol was calculated from the activation energies obtained in the range ω = 0.5–0.9 with R^2 = 0.9636–0.9826.

Curves of thermal degradation of primary coal tar distillate in the presence of nickel powder constructed by the Coats-Redfern method are showed in Figure 6.

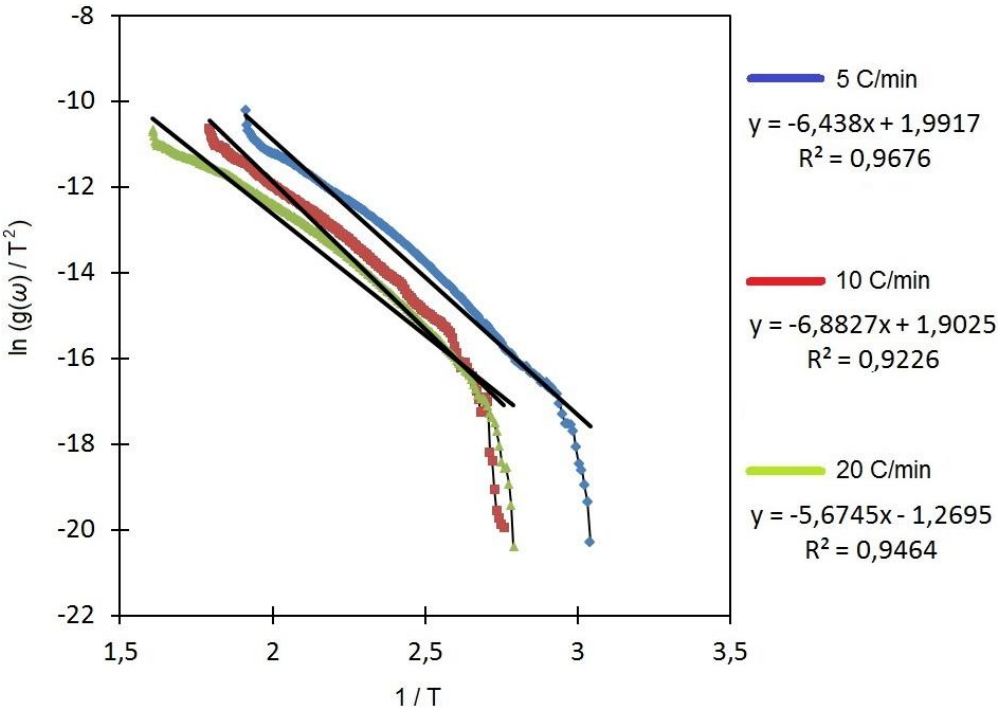

Figure 6. Curves of thermal degradation of primary coal tar distillate in the presence of nickel powder

The calculation of activation energies at different heating rates by the Coats-Redfern method is presented in Table 4.

Table 4

Calculation of activation energies at different heating rates by the Coats-Redfern method

Kinetic parameters	Without a catalyst			In the presence of nickel powder		
Heating rate (ºC/min)	5	10	20	5	10	20
Activation energy (E_a, kJ/mol)	178.753	119.185	132.203	52.525	57.22	47.18
Correlation coefficient (R^2)	0.9926	0.9909	0.9935	0.9676	0.9226	0.9446
The average value of E_a, kJ/mol	143.38			52.64		

According to the calculation received by the Coats-Redfern method for thermal degradation of primary coal tar distillate without a catalyst, the average activation energy was E_a = 143.38 kJ/mol without a catalyst and was close to activation energy value obtained by the Kissinger method.

In the presence of nickel powder the activation energy was E_a = 52.64 kJ/mol, which was close to activation energy value obtained by the FWO method.

Conclusion

The results of this study revealed that in the process of thermal degradation of primary coal tar distillate (<350 ºC) the values of activation energy calculated by model-free Kissinger and Flynn-Wall-Ozawa methods are quite consistent with model-fitting Coats-Redfern method. The differential between obtained values is insignificant. For the process of thermal degradation of primary coal tar distillate (<350 °C) without a catalyst, the calculation of the activation energy with high correlation coefficients is provided by the Kissinger and FWO methods.

The Coats-Redfern method is also suitable for calculating the activation energy in the presence of nickel nanopowder, because the obtained dependences are close to linear and have the high correlation coefficients. It was found that the addition of nanoscale nickel powder in a quantity of 1 % of distillate weight the activation energy reduces by approximately 3 times.

References

1 Zhang H. Selective hydrogenation of aromatics in coal-derived liquids over novel NiW and NiMo carbide catalysts / H. Zhang, G. Chen, L. Bai, N. Chang, Y. Wang // Fuel. — 2019. — Vol. 244. — P. 359–365. https://doi.org/10.1016/j.fuel.2019.02.015

2 Lei Z. Gas-Modified Pyrolysis Coke for in Situ Catalytic Cracking of Coal Tar / Lei, S. Hao S., Z. Lei, J. Yang // ACS Omega. — 2020. — Vol. 5. — P. 14911–14923. https://doi.org/10.1021/acsomega.0c00055

3 Baig N. Nanomaterials: a review of synthesis methods, properties, recent progress, and challenges / N. Baig, I. Kammakakam, W. Falathabe // Materials Advances. — 2020. — Vol. 2. — P. 1821–1871. https://doi.org/10.1039/D0MA00807A

4 Khalil M. Advanced nanomaterials in oil and gas industry: Design, application and challenges / M. Khalil, B.M. Jan, C.W. Tong, M.A. Berawi // Applied energy. — 2017. — Vol. 191. — P. 287–310. https://doi.org/10.1016/j.apenergy.2017.01.074

5 Suwaid M. In-situ catalytic upgrading of heavy oil using oil-soluble transition metal-based catalysts / M. Suwaid, V.A. Varfolomeev, A.A. Al-muntaser, C. Yuan, V.I. Starshinova, A. Zinnatullin, F.G. Vagizov, I.Z. Rakhmatullin, D.A. Emelian, A.E. Chemodanov // Fuel. — 2020. — Vol. 281. — Article № 118753. https://doi.org/10.1016/j.fuel.2020.118753

6 Khoshooei M.A. Activity assessment of NiMo bimetallic nanocatalyst in presence and absence of steam in in-situ upgrading technology (ISUT) / M.A. Khoshooei, S.M. Elahi, L. Carbognani, C.E. Scott // Fuel. — 2021. — Vol. 288. — Article № 119664. https://doi.org/10.1016/j.fuel.2020.119664

7 Wang W. Bifunctional catalysts for the hydroisomerization of n-alkanes: the effects of metal–acid balance and textural structure / W. Wang, C.J. Liu, W. Wu // Catalysis Science & Technology. 2019. — Vol. 9. — P. 4162–4187. https://doi.org/10.1039/C9CY00499H

8 Gang Y. Hydroprocessing of low-temperature coal tar to produce jet fuel / Y. Gang, X. Zhang, X. Lei, H. Guo, W. Li, D. Li // RSC Advances. — 2018. — Vol. 8, Issue 42. — P. 23663–23670. https://doi.org/10.1039/C8RA04531C

9 Kan T. Production of Gasoline and Diesel from Coal Tar via Its Catalytic Hydrogenation in Serial Fixed Beds / T. Kan, X. Sun, H. Wang, C. Li, U. Muhammad // Energy & Fuels. — 2012. — Vol. 26, Issue 6. — P. 3604−3611. https://doi.org/10.1021/EF3004398

10 Qi S.C. A highly active Ni/ZSM-5 catalyst for complete hydrogenation of polymethylbenzenes / S.C. Qi, X.Y. Wei, Z.M. Zong, J.I. Hayashi, X.H. Yuan, L.B. Sun L.B. // ChemCatChem. — 2013. — Vol. — 5, Issue 12. — P. 3543–3547. https://doi.org/10.1002/cctc.201300547

11 Maloletnev A.S. Refining of coal tar by hydrogenation in the presence of nanoheterogeneous nickel sulfide catalyst / A.S. Maloletnev, Zh.K. Kairbekov, N.T. Smagulova // Coke and Chemistry. — 2020. — Vol. 63, Issue 5. — P. 253–256. https://doi.org/10.3103/S1068364X20050038

12 Baikenov M.I. Effect of new catalytic systems on the process of anthracene hydrogenation / M.I. Baikenov, G.G. Baikenova, A.S. Isabaev, A.B. Tateeva, Zh.S. Akhmetkarimova, A. Tusipkhan, A.Zh. Mataeva, K.K. Esenbaeva // Solid fuel chemistry. — 2015. — Vol. 49. — P. 150–155. https://doi.org/10.3103/S0361521915030039

13 Baikenov M.I. Hydrogenation of polyaromatic compounds over NiCo/chrysotile catalyst / M.I. Baikenov, D.E. Aitbekova, N.Zh. Balpanova, A. Tusipkhan, G.G. Baikenova, Y.A. Aubakirov, A.R. Brodskiy, F. Ma, D.K. Makenov // Bulletin of the University of Karaganda — Chemistry. — 2021. — Vol. 103, № 3. — P. 74–82. https://doi.org/10.31489/2021Ch3/74-82

14 Balpanova N.Zh. Thermokinetic parameters of the primary coal tars destruction in the presence of catalysts and polymeric materials / N.Zh. Balpanova, M.I. Baikenov, A.M. Gyulmaliev, Z.B. Absat, Zh. Batkhan, F. Ma, K. Su, S.V. Kim, G.G. Baikenova, D.E. Aitbekova, A. Tusipkhan // Bulletin of the University of Karaganda — Chemistry. — 2021. — Vol. 102, № 2. — P. 86–95. https://doi.org/10.31489/2021Ch2/86-95

15 Kim S.V. Catalytic properties of ultrafine nickel powder in the hydrogenation of anthracene and phenanthrene / S.V. Kim, K.S. Ibishev, M.I. Baikenov, A. Tusipkhan, V.P. Grigor'eva & A.M. Gyul'maliev // Solid fuel chemistry. — 2022. — Vol. 56. — P. 53-58. https://doi.org/10.3103/S0361521922010025

16 Vyazovkin S. ICTAC Kinetics Committee recommendations for performing kinetic computations on thermal analysis data / S. Vyazovkin, A.K. Burnham, J.M. Criado, L.A. Pérez-Maqueda, C. Popescu, N. Sbirrazzuoli // Thermochimica Acta. — 2011. — Vol. 520. — P. 1–19. https://doi.org/10.1016/j.tca.2011.03.034

17 Chun Minh Loy A. Thermogravimetric kinetic modelling of 1 in-situ catalytic pyrolytic conversion of rice husk to bioenergy using rice hull ash catalyst / A. Chun Minh Loy, D. Kin Wai Gan, S. Yusup, B. Lai Fui Chin, M.K Lam, M. Shahbaz, P. Unrean, M.N. Acda, E. Rianawati // Bioresource Technology. — 2018. — Vol. 261. — P. 213–222. https://doi.org/10.1016/j.biortech.2018.04.020

18 Heydari M. Kinetic Study and Thermal Decomposition Behavior of Lignite Coal / M. Heydari, M. Rahman, R. Gupta // International Journal of Chemical Engineering. — 2015. — Article ID 481739. https://doi.org/10.1155/2015/481739

19 Yao Z. Comparative study on the pyrolysis kinetics of polyurethane foam from waste refrigerators. / Z. Yao, S. Yu, W. Su, W. Wu, J. Tang, W. Qi // Waste Management & Research. — 2019. — Vol. 38, Issue 3. — P. 271–278. https://doi.org/10.1177/0734242X19877682

20 Balart R. Kinetic analysis of the thermal degradation of recycled acrylonitrile-butadiene-styrene by non-isothermal thermogravimetry / R. Balart, D. Garcia-Sanoguera, L. Quiles-Carrillo, N. Montanes, G. Torres-Giner // Polymers. — 2019. — Vol. 11, Issue 2. — Article № 281. https://doi.org/10.3390/polym11020281

21 Kozlov A.N. A kinetic analysis of the thermochemical conversion of solid fuels (A Review) / A.N. Kozlov, D.A. Svishcheva, D.I. Khudiakova, A.F. Ryzhkov // Solid Fuel Chemistry. — 2017. — Vol. 51, Issue 4. — P. 205–213. https://doi.org/10.3103/S0361521917040061

С.В. Ким, М.И. Байкенов, К.С. Ибишев,
М.Г. Мейрамов, Фен Юн Ма, Т.О. Хамитова

Таскөмір шайыры дистиллятының термиялық ыдырауына никель наноұнтағының әсері

Таскөмір шайыры дистиллятының термиялық ыдырау процесіне никель наноұнтағының әсер ету заңдылықтары Киссинджер, Флинн-Уолл-Озава динамикалық модельсіз әдістерін және Коутс-Редферн модельді әдісін қолдана отырып анықталды. Қайнау температурасы <350 °С болатын таскөмір шайырының дистилляты Шұбаркөл кен орнының біріншілік таскөмір шайырын қарапайым айдау арқылы алынды. Катализатор ретінде қолданылған наноөлшемді никель ұнтағы таскөмір шайырының дистилляты массасына 1 % мөлшерде қосылды, содан кейін таскөмір шайыры дистиллятының термиялық ыдырау процесі инертті газ ортасында 5, 10 және 20 °С/мин қыздыру жылдамдықтарымен жүргізілді. Никель ұнтағы электролиз процесіне тұрақты токта жоғары вольтты разрядпен әсер еткен кезде алынды. Рентгендік фазалық анализ (РФА) алынған никель ұнтағы қырлы орталықтанған текше құрылымды екенін көрсетті, ал Шеррер теңдеуімен есептелген кристаллиттердің орташа өлшемі шамамен 34 нм құрады. Активтелу энергиясын есептеу термогравиметриялық мәліметтерді өңдеу арқылы жүргізілді. Киссинджер әдісі бойынша есептеу активтелу энергиясының мәні 145,19 кДж/моль-ден 43,65 кДж/моль-ге дейін төмендейтінін көрсетті, Флинн-Уолл-Озава (FWO) әдісі бойынша активтелу энергиясының мәні 152,82 кДж/моль-ден 51,65 кДж/моль-ге дейін төмендейтіні анықталды және Коутс-Редферн модельдік әдісіне сәйкес активтелу энергиясының мәні 143,38 кДж/моль-ден 52,64 кДж/моль-ге дейін төмендейді. Алынған корреляция коэффициенттерінің жоғары мәндері бұл әдістердің қолданылу мүмкіншілігін анықтайды.

Кілт сөздері: термиялық деструкция, никель, наноұнтақ, таскөмір шайыры, дистиллят, кристаллит, термогравиметриялық анализ, активтелу энергиясы.

С.В. Ким, М.И. Байкенов, К.С. Ибишев,
М.Г. Мейрамов, Фен Юн Ма, Т.О. Хамитова

Влияние нанопорошка никеля на термическое разложение дистиллята каменноугольной смолы

Закономерности влияния нанопорошка никеля на процесс термического разложения дистиллята каменноугольной смолы были определены с использованием динамических безмодельных методов Киссинджера, Флинна-Уолла-Озавы и модельного метода Коутса-Редферна. Дистиллят каменноугольной смолы с температурой кипения < 350 °С был получен простой перегонкой первичной каменноугольной смолы с месторождения Шубарколь. В качестве катализатора использовали наноразмерный порошок никеля, который добавляли в дистиллят каменноугольной смолы в количестве 1 % от массы дистиллята и затем проводили процесс термической деструкции дистиллята каменноугольной смолы при скоростях нагрева 5, 10 и 20 °С/мин в среде инертного газа. Порошок никеля был получен при воздействии высоковольтного разряда на процесс электролиза на постоянном токе. Проведенный рентгенофазовый анализ (РФА) показал, что полученный порошок никеля имеет гранецентрированную кубическую структуру, а средний размер кристаллитов, рассчитанный по уравнению Шеррера, составил примерно 34 нм. Расчеты энергии активации проводились с помощью обработки термогравиметрических данных. Расчет по методу Киссинджера показал, что значение энергии активации уменьшается с 145,19 кДж/моль до 43,65 кДж/моль, по методу Флинна-Уолла-Озавы (FWO) установлено, что значение энергии активации уменьшается с 152,82 кДж/моль до 51,65 кДж/моль и согласно модельному методу Коутса-Редферна значение энергии активации уменьшается со 143,38 кДж/моль до 52,64 кДж/моль. Применимость данных методов обеспечивается полученными высокими значениями коэффициентов корреляции.

Ключевые слова: термическая деструкция, никель, нанопорошок, каменноугольная смола, дистиллят, кристаллит, термогравиметрический анализ, энергия активации.

References

1 Zhang H., Chen G., Bai L., Chang N., Wang Y. (2019). Selective hydrogenation of aromatics in coal-derived liquids over novel NiW and NiMo carbide catalysts. *Fuel, 244,* 359–365.

2 Lei Z., Hao S., Lei Z., Yang J. Gas-Modified Pyrolysis Coke for in Situ Catalytic Cracking of Coal Tar. (2020). *ACS Omega, 5,* 14911–14923.

3 Baig N., Kammakakam I., Falathabe W. (2021). Nanomaterials: a review of synthesis methods, properties, recent progress, and challenges. *Materials Advances, 2,* 1821–1871.

4 Khalil M., Jan B.M., Tong C.W., Berawi M.A (2017). Advanced nanomaterials in oil and gas industry: Design, application and challenges. *Applied energy, 191,* 287–310.

5 Suwaid M., Varfolomeev V.A., Al-muntaser A.A., Yuan C., Starshinova V.I., Zinnatullin A., Vagizov F.G., Rakhmatullin I.Z., Emelian D.A., Chemodanov A.E. (2020). In-situ catalytic upgrading of heavy oil using oil-soluble transition metal-based catalysts. *Fuel, 281,* 118753.

6 Khoshooei M.A., Elahi S.M., Carbognani L., Scott C.E. (2021). Activity assessment of NiMo bimetallic nanocatalyst in presence and absence of steam in in-situ upgrading technology (ISUT) *Fuel, 288,* 119664.

7 Wang W., Liu C.J., Wu W. (2019). Bifunctional catalysts for the hydroisomerization of *n*-alkanes: the effects of metal–acid balance and textural structure. *Catalysis Science & Technology, 9,* 4162–4187.

8 Gang Y., Zhang X., Lei X., Guo H., Li W., Li D. (2018). Hydroprocessing of low-temperature coal tar to produce jet fuel. *RSC Advances, 8(42),* 23663–23670.

9 Kan T., Sun X., Wang H., Li C., Muhammad U. (2012). Production of Gasoline and Diesel from Coal Tar via Its Catalytic Hydrogenation in Serial Fixed Beds. *Energy & Fuels, 26(6),* 3604−3611.

10 Qi S.C., Wei X.Y., Zong Z.M., Hayashi J.I., Yuan X.H., Sun L.B. (2013). A highly active Ni/ZSM-5 catalyst for complete hydrogenation of polymethylbenzenes. *ChemCatChem, 5(12),* 3543–3547.

11 Maloletnev A.S., Kairbekov Zh.K., Smagulova N.T. (2020). Refining of coal tar by hydrogenation in the presence of nanoheterogeneous nickel sulfide catalyst. *Coke and Chemistry, 63(5),* 253–256. [(2020). Гидрооблагораживание каменноугольной смолы в присутствии наногетерогенных никельсульфидных катализаторов. *Кокс и химия, 5,* 45–49].

12 Baikenov M.I., BaikenovaG.G., Isabaev A.S., Tateeva A.B., Akhmetkarimova Zh.S., Tusipkhan A., Mataeva A.Zh., Esenbaeva K.K. Effect of new catalytic systems on the process of anthracene hydrogenation. (2015). *Solid fuel chemistry, 49,* 150–155. [(2015). Влияние новых каталитических систем на процесс гидрогенизации антрацена. *Химия твердого топлива, 3,* 22–27].

13 Baikenov M.I., Aitbekova D.E., Balpanova N.Zh, Tusipkhan A., Baikenova G.G., Aubakirov Y.A., Brodskiy A.R., Ma F., Makenov D.K. Hydrogenation of polyaromatic compounds over NiCo/chrysotile catalyst. (2021). *Bulletin of the University of Karaganda — Chemistry, 103(3),* 74–82.

14 Balpanova N.Zh., Baikenov M.I., Gyulmaliev A.M., Absat Z.B., Batkhan Zh., Ma F., Su K., Kim S.V., Baikenova G.G., Aitbekova D.E., Tusipkhan A. (2021). Thermokinetic parameters of the primary coal tars destruction in the presence of catalysts and polymeric materials. *Bulletin of the University of Karaganda — Chemistry, 102(2),* 86–95.

15 Kim S.V., Ibishev K.S., Baikenov M.I., Tusipkhan A., Grigor'eva V.P., Gyul'maliev A.M. (2022). Catalytic properties of ultrafine nickel powder in the hydrogenation of anthracene and phenanthrene. *Solid fuel chemistry, 56,* 53-58. [(2022). Каталитические свойства ультрадисперсного порошка никеля при гидрогенизации антрацена и фенантрена. *Химия твердого топлива, 1,* 36–42].

16 Vyazovkin S., Burnham A.K., Criado J.M., Pérez-Maqueda L.A., Popescu C., Sbirrazzuoli N. (2011). ICTAC Kinetics Committee recommendations for performing kinetic computations on thermal analysis data. *Thermochimica Acta, 520,* 1–19.

17 Chun Minh Loy A., Kin Wai Gan D., Yusup S., Lai Fui Chin B., Lam M.K, Shahbaz M., Unrean P.5, Acda M.N., Rianawati E. (2018). Thermogravimetric kinetic modelling of 1 in-situ catalytic pyrolytic conversion of rice husk to bioenergy using rice hull ash catalyst. *Bioresource Technology, 261,* 213–222.

18 Heydari M., Rahman M., Gupta R. (2015). Kinetic Study and Thermal Decomposition Behavior of Lignite Coal. (2015). *International Journal of Chemical Engineering, 2015,* Article ID 481739.

19 Yao Z., Yu S., Su W., Wu W., Tang J., Qi W. (2019). Comparative study on the pyrolysis kinetics of polyurethane foam from waste refrigerators. *Waste Management & Research, 38(3),* 271–278.

20 Balart R., Garcia-Sanoguera D., Quiles-Carrillo L., Montanes N., Torres-Giner G. (2019). Kinetic analysis of the thermal degradation of recycled acrylonitrile-butadiene-styrene by non-isothermal thermogravimetry. *Polymers, 11(2), 281,* 1–23.

21 Kozlov A.N., Svishcheva D.A., Khudiakova D.I., Ryzhkov A.F. (2017). A kinetic analysis of the thermochemical conversion of solid fuels (A Review). *Solid Fuel Chemistry, 51(4),* 205–213. [(2017). Кинетический анализ термохимической конверсии твердых топлив. *Химия твердого топлива, 4,* 12–21].

Information about authors

Kim, Sergey Valerievich (corresponding author) — Doctoral student, Karagandy University of the name of academician E.A. Buketov, Universitetskaya street, 28, 100024, Karaganda, Kazakhstan; research engineer, Abishev Chemical-Metallurgical Institute, Karaganda, Ermekov street, 63, 100009, Kazakhstan; e-mail: vanquishV8@mail.ru; https://orcid.org/0000-0002-6044-9438;

Baikenov, Murzabek Ispolovich — Doctor of chemical sciences, Professor, Karagandy University of the name of academician E.A. Buketov, Universitetskaya street, 28, 100024, Karaganda, Kazakhstan; e-mail: murzabek_b@mail.ru; https://orcid.org/0000-0002-8703-0397;

Ibishev, Kanat Sansyzbaevich — Candidate of chemical sciences, Leading researcher, Abishev Chemical-Metallurgical Institute, Karaganda, Ermekov street, 63, 100009, Kazakhstan; e-mail: ikanat2014@mail.ru; https://orcid.org/0000-0001-7622-2791;

Meiramov, Mazhit Gabdullovich — Candidate of chemical sciences, Senior researcher, Institute of Organic Synthesis and Coal Chemistry, Karaganda, Alihanova street, 1, 100008, Kazakhstan; e-mail: majit_m@mail.ru; https://orcid.org/0000-0003-2498-6516;

Ma, Fengyun — PhD, professor, Xinjiang University, Urumqi, Nan Min Lu street, 666, Xinjiang Uygur Autonomous Region (XUAR) People's Republic of China (PCR); e-mail: ma_fy@126.com;

Khamitova, Tolkyn Ondirisovna — PhD, Agronomic Faculty, Kazakh Agro Technical University named after Saken Seifullin, Nur-Sultan, Zhenis avenue, 62, 010011, Kazakhstan; e-mail: khamitova.t@inbox.ru; https://orcid.org/0000-0002-4691-3732